Neurobiology of Disease

Synergistic Interactions between Aβ, Tau, and α-Synuclein: Acceleration of Neuropathology and Cognitive Decline

Lani K. Clinton,[1]* Mathew Blurton-Jones,[1]* Kristoffer Myczek,[1]* John Q. Trojanowski,[2] and Frank M. LaFerla[1]

[1]Department of Neurobiology and Behavior, University of California, Irvine, Irvine, California 92697-4545, and [2]Center for Neurodegenerative Disease Research, Department of Pathology and Laboratory Medicine, University of Pennsylvania School of Medicine, Philadelphia, Pennsylvania 19104

Alzheimer's disease (AD), the most prevalent age-related neurodegenerative disorder, is characterized pathologically by the accumulation of β-amyloid (Aβ) plaques and tau-laden neurofibrillary tangles. Interestingly, up to 50% of AD cases exhibit a third prevalent neuropathology: the aggregation of α-synuclein into Lewy bodies. Importantly, the presence of Lewy body pathology in AD is associated with a more aggressive disease course and accelerated cognitive dysfunction. Thus, Aβ, tau, and α-synuclein may interact synergistically to promote the accumulation of each other. In this study, we used a genetic approach to generate a model that exhibits the combined pathologies of AD and dementia with Lewy bodies (DLB). To achieve this goal, we introduced a mutant human α-synuclein transgene into 3xTg-AD mice. As occurs in human disease, transgenic mice that develop both DLB and AD pathologies (DLB-AD mice) exhibit accelerated cognitive decline associated with a dramatic enhancement of Aβ, tau, and α-synuclein pathologies. Our findings also provide additional evidence that the accumulation of α-synuclein alone can significantly disrupt cognition. Together, our data support the notion that Aβ, tau, and α-synuclein interact *in vivo* to promote the aggregation and accumulation of each other and accelerate cognitive dysfunction.

Introduction

β-Amyloid (Aβ), tau, and α-synuclein (α-syn) are the primary components of amyloid plaques, neurofibrillary tangles, and Lewy bodies (LBs), respectively. Many neurodegenerative disorders are characterized by the presence of one or more of these lesions. For example, "pure" Alzheimer's disease (AD) is epitomized by the accumulation of Aβ plaques and neurofibrillary tangles. Patients with the most common subtype of AD, the Lewy body variant of AD (DLB-AD), also exhibit α-syn-bearing LBs. Interestingly, up to 50% of AD cases exhibit significant LB pathology in addition to plaques and tangles (Raghavan et al., 1993; Hamilton, 2000; Postina, 2008). Such examples of "triple brain amyloidosis" are increasingly being identified postmortem (Trojanowski, 2002). Patients with DLB-AD typically exhibit a more aggressive disease course and more pronounced cognitive dysfunction than patients with pure AD (Hansen et al., 1990; Langlais et al., 1993; Olichney et al., 1998; Kraybill et al., 2005). Importantly, plaques, tangles, and LBs do not develop in high enough individual frequency to explain their co-occurrence simply by statistical overlap; thus, it has been hypothesized that Aβ, tau, and α-syn promote the accumulation of one another (Giasson et al., 2003; Lee et al., 2004).

Received Jan. 28, 2010; accepted March 16, 2010.

This work was supported by National Institutes of Health (NIH)–National Institute on Aging (NIA) Grants R01 AG027544 (F.M.L.), T32 AG00096 (L.K.C., K.M.), and K01 AG029378 (M.B.-J.), and Udall Center Grant NS-053488 (J.Q.T.). Aβ peptides and anti-Aβ antibodies were provided by the University of California Alzheimer's Disease Research Center NIH–NIA Grant P50 AG16573. Special thanks to Virginia M. Lee and Kim N. Green for collaboration and advice.

*L.K.C., M.B.-J., and K.M. contributed equally to this work.

Correspondence should be addressed to Dr. Frank M. LaFerla, Department of Neurobiology and Behavior, 1109 Gillespie Neuroscience Research Facility, University of California, Irvine, Irvine, CA 92697-4545. E-mail: laferla@uci.edu.

DOI:10.1523/JNEUROSCI.0490-10.2010

 0270-6474/10/307281-09$15.00/0

A growing number of studies support this hypothesis. For example, α-syn aggregates in a concentration-dependent manner but fails to form fibrils at lower concentrations unless coincubated with tau (Giasson et al., 2003). This relationship appears reciprocal, as α-syn can likewise promote tau polymerization (Giasson et al., 2003; Kotzbauer et al., 2004). α-syn may also promote tau accumulation *in vivo*. For example, one member of the Contursi kindred, a family with familial Parkinson's disease associated with the $\alpha\text{-syn}_{A53T}$ mutation, exhibits tangle pathology in addition to LBs (Giasson et al., 2003; Kotzbauer et al., 2004). A small percentage of M83 $\alpha\text{-syn}_{A53T}$ transgenic mice also exhibit tau inclusions (Giasson et al., 2003). Interestingly, Aβ also appears to influence α-syn and tau aggregation. Double-transgenic α-syn/amyloid precursor protein (APP) mice exhibit increased α-syn deposition versus single-transgenic mice (Masliah et al., 2001), and Aβ and α-syn may interact directly to form cation channels that contribute to neurodegeneration (Tsigelny et al., 2008). Evidence from our own laboratory also suggests a hierarchical relationship between Aβ and tau accumulation (Oddo et al., 2004).

Our laboratory previously generated the 3xTg-AD mouse model of AD that develops both Aβ plaques and neurofibrillary tangles (Oddo et al., 2003). However, a transgenic model of DLB-AD that exhibits all three proteinopathies has not yet been developed. Given the prevalence of DLB-AD as a predominate variant of AD and the relationship of LBs to other common neurodegenerative disorders such as Parkinson's disease and Lewy Body disease, we sought to generate a transgenic model of DLB-AD. To achieve this goal we crossed 3xTg-AD mice with mice that express the A53T mutation in α-syn (Giasson et al., 2002). This transgenic line, hereafter referred to as DLB-AD mice, provides a unique opportunity to elucidate the complex interactions between Aβ, tau, and α-syn *in vivo*. Importantly, these mice also

allow us to examine the combined impact of triple brain amyloidosis on cognitive function.

Materials and Methods

Mice. 3xTg-AD mice have previously been characterized (Oddo et al., 2003; Billings et al., 2005). Briefly, the mice were generated by microinjecting two transgenes expressing human APP with the Swedish mutation (KM670/671NL) and human tau with the P301L mutation into single-cell embryos of homozygous $PS1_{M146V}$ knock-in mice. The original hybrid background strain of 3xTg-AD and control mice is 129/C57BL6. M83-h transgenic α-syn_{A53T} mice have also previously been well characterized (Giasson et al., 2002). These mice express human α-syn with the A53T mutation under regulatory control of the mouse prion promoter and are maintained on a C57BL/6/C3H background. Male and female mice were individually housed unless used for breeding and kept on a 12 h light/dark schedule with *ad libitum* access to food and water. All groups of mice used in this study were derived using a minimum set of crosses (three) to minimize potential genetic drift. In addition, mice were derived such that the C57BL/6/C3H/129 mixed background strain was equivalent between DLB-AD, 3xTg-AD, α-syn, and nontransgenic (non-Tg) groups (see supplemental Fig. 1, Table 1, available at www.jneurosci.org as supplemental material). Male and female mice were used for this study and groups were matched for both sex and age. Animals were maintained, and all experiments were performed in strict accordance to institutional regulations regarding animal use.

Barnes circular maze. In a previous study, we found that 3xTg-AD mice exhibit sex differences in Morris water maze performance because of a differential stress response (Clinton et al., 2007). To achieve a reasonable sample size for this study, we needed to use both male and female transgenic mice in age- and sex-matched groups. We therefore chose to use the Barnes maze, a less stressful measure of spatial memory. The apparatus used for all Barnes maze tasks was an elevated circular platform (1 m diameter) with 40 holes (5 cm diameter) around the perimeter of the platform, one of which was connected to an escape chamber (Columbus Instruments) in a room with simple, extramaze visual clues. Before the first day of training, mice were habituated to the testing room for 1 h in their home cages.

Training consisted of four trials per day for 4 d separated by a 15 min intertrial interval. Each mouse was placed in the center of the maze under a start box. On the first trial, when the start box was lifted, the mouse was allowed 5 min to locate the escape chamber; all subsequent trials were 2 min long. If the mouse failed to find the escape chamber at the end of the first trial, it was gently guided to the escape chamber and allowed to remain there for 60 s to orient the mouse to the existence of the escape chamber. The location of the escape box was randomly selected as one of three locations in the room (designated as A, B, or C), but the location of the escape chamber was kept consistent for each individual animal. The parameters measured during training included (1) latency to find escape chamber, (2) latency to enter escape chamber, and (3) the number of errors or incorrect hole pokes. An animal was considered to find the escape chamber when the animal's nose crossed the horizontal plane of the platform. The same criterion was used to record the number of errors. An animal was considered to enter the escape chamber when the animal's entire body was in the escape chamber and no longer visible on the platform. Retention was tested 24 h and 7 d after the fourth day of training. Both retention trials consisted of a single 2 min trials with the escape chamber present. The parameters measured were identical with those collected during training.

Inhibitory avoidance. Testing began with a single training trial in which the mouse was placed in a lighted chamber; when the mouse crossed over to the dark chamber, it received a mild (0.2 mA/1 s) footshock. This initial latency to enter the dark (shock) compartment served as the baseline measure. At 1.5 or 24 h after training, probe trials were performed; the mouse was again placed in the light compartment, and the latency to return to the dark compartment was measured as an index of inhibitory avoidance (IA).

Accelerating rotarod. To test general motor ability, mice were trained on an accelerating rotarod (Columbus). First, mice were required to balance on the stationary rod for 30 s before training began. Training consisted of four 60 s trials with an intertrial interval of 30 s. The initial speed of the rotarod was set at 4 rotations per minute (rpm) with an acceleration of 0.2 rpm. After 2 d of training, the mice were tested. Testing consisted of four 120 s trials with an intertrial interval of 30 s. The initial speed of the rotarod was the same as training (4 rpm); however, the acceleration was more rapid at 0.3 rpm. The parameter measured was the time at which the mouse fell from the rotating rod. This time was converted into rpm to determine how fast the rod was rotating at the time of fall as follows: rpm at time of fall = initial speed + (acceleration * latency to fall).

Immunohistochemistry. Mice were killed by CO_2 asphyxiation, and the brains were rapidly removed and fixed for 48 h in 4% paraformaldehyde, pH 7.4. Free-floating 40-μm-thick sagittal sections were collected on a freezing microtome and stored in 0.01 M PBS with 0.02% NaN_3. Primary antibodies used included the following: antibodies against Aβ: 6E10 (Signet; diluted 1:1000), OC (gift from C. Glabe, University of California, Irvine, CA); tau and phospho-tau: HT7 (Innogenetics; diluted 1:1000), AT8 (phosphoserine 202 and 205; Innogenetics; diluted 1:200); α-syn: AB5038 (Millipore Bioscience Research Reagents; diluted 1:1000); and α-syn: ab16784 (Abcam; diluted 1:10,000). Primary antibodies were applied overnight at 4°C, and labeling was visualized with the Vector ABC DAB system. For immunofluorescent labeling and confocal microscopy, methods followed previously established protocols (Blurton-Jones and Tuszynski, 2006; Yamasaki et al., 2007). Briefly, primary antibodies were detected by incubating with appropriate Alexa Fluor fluorescent secondary antibodies (Invitrogen) for 1 h at room temperature. Immunofluorescence was visualized using the Bio-Rad 2100 confocal imaging system (Bio-Rad Laboratories). To avoid nonspecific bleedthrough, each laser line was excited and detected independently using lambda-strobing mode. Images represent either single confocal *Z*-slices or *Z*-stacks.

Biochemical analysis. Brains were rapidly frozen after removal from the skull and stored at −80°C until they were processed for biochemistry. Whole brains (excluding the cerebellum) were solubilized with T-PER (Pierce) with Complete mini-protease inhibitor (Roche) and phosphatase inhibitor mixtures (Sigma-Aldrich). The homogenate was spun at 35,000 rpm for 1 h at 4°C in a T865 Sorvall rotor in a L8-70 ultracentrifuge (Beckman Coulter). The supernatant was collected and stored at −80°C. The pellet was resuspended in 70% formic acid (FA) and spun as in the previous step. The supernatant was collected and stored at −80°C. FA fractions for insoluble Western blots were diluted 1:3 with a 1:1 mixture of 10N NaOH and neutralization buffer (1 mol/L Tris base; 0.5 mol/L NaH_4PO_4). Western blots were then performed using standard protocols. Soluble and insoluble levels of $A\beta_{40}$ and $A\beta_{42}$ were also measured by sandwich ELISA as previously described (Billings et al., 2005; Oddo et al., 2006).

Statistics. For behavior tests, we used a repeated-measure ANOVA with a *post hoc* Bonferroni including age and genotype on the Barnes circular maze (BCM), IA, and rotarod acquisition, retention, and probe trials. ANOVA or *t* test comparisons were used to determine differences in ELISA, Western blot, and plaque count quantification using StatView software. Data were considered to be significant when $p < 0.05$.

Results

Generation and motor performance of DLB-AD mice

To generate a mouse model of DLB-AD, we crossed homozygous 3xTg-AD mice to hemizygous α-syn_{A53T}-expressing mice (M83-h line) and performed repeated backcrossing and genotyping to restore homozygosity for the $presenilin_{M146V}$, APP_{swe}, and Tau_{p301L} transgenes and establish hemizygosity for the α-syn_{A53T} transgene. The resultant mice, herein referred to as DLB-AD mice, were then compared with 3xTg-AD, M83-h α-syn single-transgenic, and wild-type groups that had been generated concurrently on the same mixed background strain (supplemental Fig. 1, available at www.jneurosci.org as supplemental material). Hemizygous single-transgenic M83 (M83-h) mice typically develop motor deficits at 22–28 months, whereas homozygous M83 (M83-H) mice develop motor deficits between 8 and 16 months of age (Giasson et al., 2002). We therefore maintained the α-syn transgene in a hemizygous state, with the goal of testing cognitive function without the potential confound of motor impairment.

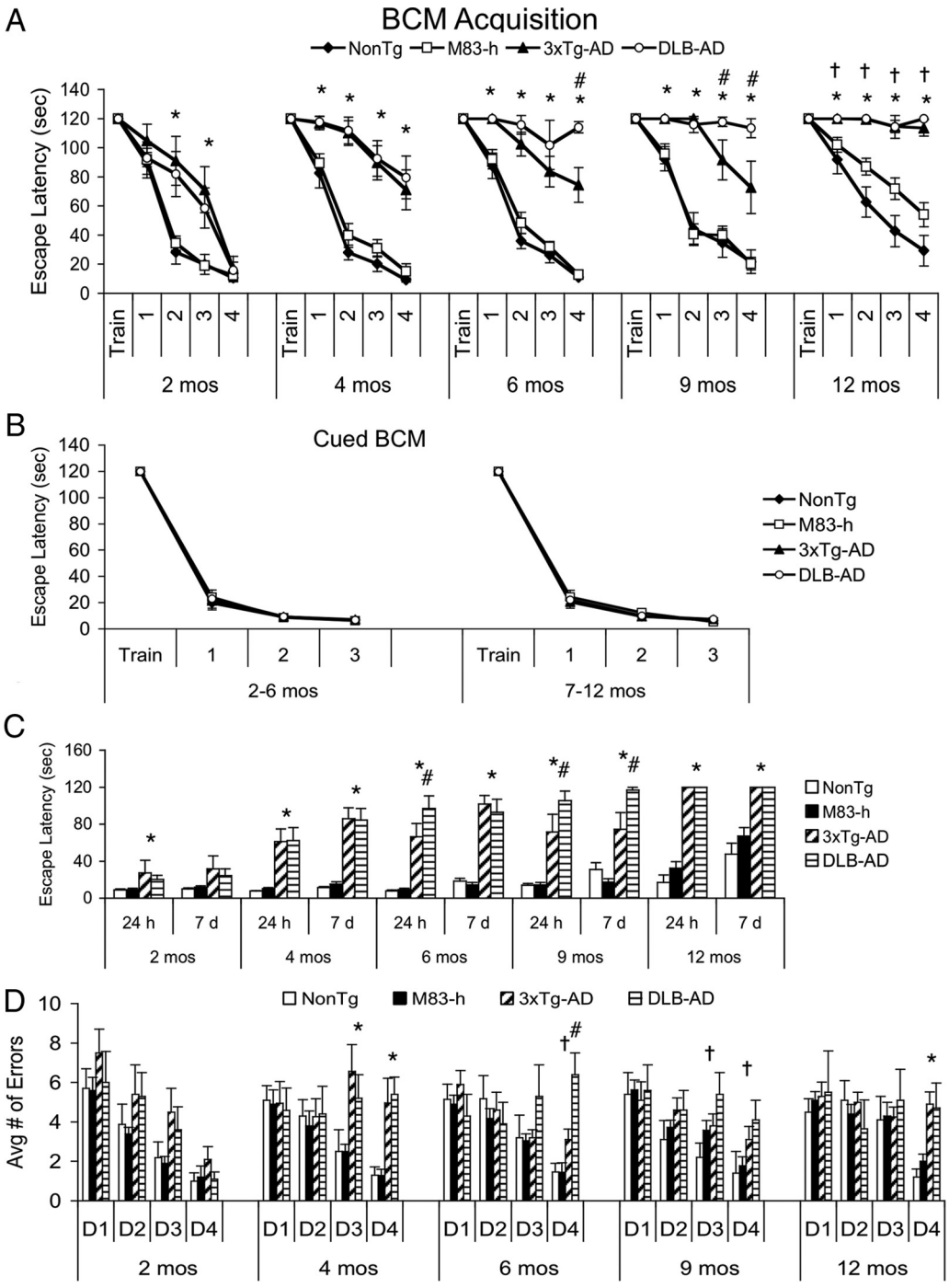

Figure 1. Coexpression of α-syn, Aβ, and tau accelerates cognitive decline in DLB-AD mice. ***A***, BCM acquisition. DLB-AD mice exhibit accelerated cognitive decline during BCM acquisition. Two-month-old 3xTg-AD and DLB-AD mice have significantly longer escape latencies than non-Tg and M83-h mice on days 2 and 3 of acquisition ($^{*}p < 0.05$). Four-, 6-, 9-, and 12-month-old 3xTg-AD and DLB-AD are significantly worse than non-Tg and M83-h mice on all 4 d of acquisition ($^{*}p < 0.05$). An interesting difference emerges between the 3xTg-AD and DLB-AD mice at 6 months of age whereby the DLB-AD mice have significantly longer group escape latency on day 4 of acquisition ($^{\#}p < 0.05$). This difference is further exacerbated at 9 months of age when the DLB-AD mice have significantly longer escape latencies than age-matched 3xTg-AD mice on days 3 and 4 of acquisition ($^{\#}p < 0.05$), but this difference is no longer evident at 12 months of age ($p > 0.05$). Interestingly, 12-month-old M83-h mice are significantly impaired compared with age-matched non-Tg mice on all 4 d of acquisition ($^{\dagger}p < 0.05$), supporting the notion that mutant α-syn alone can disrupt cognition. ***B***, No genotype differences were apparent on the cued BCM. Both young (2–6 months) and older (7–12 months) perform equivalently on the cued version of the BCM ($p > 0.05$). ***C***, Retention trials. 3xTg-AD and DLB-AD mice have significantly longer escape latencies on both the 24 h and 7 d retention trials compared with age-matched non-Tg and M83-h mice at 4, 6, 9, and 12 months of age ($^{*}p < 0.05$). 3xTg-AD and DLB-AD mice are significantly impaired compared with non-Tg and M83-h at the 24 h retention at 2 months of age but are unimpaired on the 7 d retention trial. Six-month-old DLB-AD mice are significantly impaired compared with age-matched 3xTg-AD mice at the 24 h retention trial ($^{\#}p < 0.05$), and 9-month-old DLB-AD have significantly worse short- and long-term retention compared with age-matched 3xTg-AD mice ($^{\#}p < 0.05$). ***D***, Errors made during BCM acquisition. There are no significant genotype differences at 2 months of age ($p > 0.05$). Four-month-old 3xTg-AD and DLB-AD mice visit significantly more incorrect holes compared with age-matched non-Tg and M83-h mice ($^{*}p < 0.05$). Six-month-old DLB-AD make significantly more errors compared with age-matched 3xTg-AD mice on day 4 ($^{\#}p < 0.05$) and age-matched non-Tg and M83-h mice on day 4 ($^{\dagger}p < 0.05$). Nine-month-old DLB-AD mice make significantly more errors than non-Tg and M83-h mice on days 3 and 4 ($^{\dagger}p < 0.05$). Twelve-month-old 3xTg-AD and DLB-AD mice visit significantly more incorrect holes than age-matched non-Tg and M83-h mice ($^{*}p < 0.05$). Error bars indicate SEM.

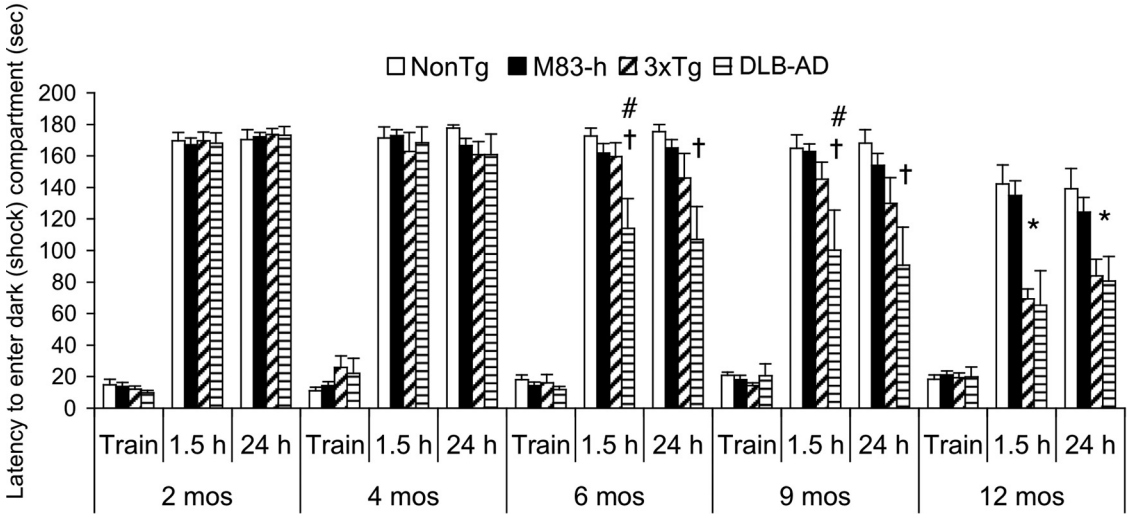

Figure 2. DLB-AD exhibit deficits in an inhibitory avoidance task at earlier ages than 3xTg-AD, M83-h, and control mice. All genotypes are unimpaired at 2 and 4 months of age. Six-month-old DLB-AD mice cross over to the dark (shock) compartment significantly faster compared with age-matched 3xTg-AD mice ($^{\#}p < 0.05$) and non-Tg/M83-h mice ($^{\dagger}p < 0.05$) at the 1.5 h probe trial. Nine-month-old DLB-AD mice cross over to the dark (shock) compartment significantly faster compared with age-matched 3xTg-AD mice ($^{\#}p < 0.05$) and non-Tg/M83-h mice ($^{\dagger}p < 0.05$) at both the 1.5 and 24 h probe trial. Twelve-month-old 3xTg-AD and DLB-AD mice have significantly impaired short- and long-term retention compared with age-matched non-Tg and M83-h mice ($^{*}p < 0.05$). Error bars indicate SEM.

However, to verify that DLB-AD mice exhibit no motor deficits at the ages studied (2–12 months), we examined motor function with an accelerating rotarod task. All genotypes (non-Tg, M83-h, 3xTg-AD, and DLB-AD) were examined at 2, 4, 6, 9, and 12 months of age, and no differences in either female or male weight were detected (data not shown). Importantly, at each of these ages, we also found no motor deficits in any of the four genotypes tested (supplemental Fig. 2, available at www.jneurosci.org as supplemental material).

Coexpression of α-syn accelerates the development of AD-related cognitive deficits

We previously showed that 3xTg-AD mice develop progressive, age-related deficits in spatial memory and fear conditioning (Billings et al., 2005). However, it remains unknown whether α-syn can alter the development of AD-related cognitive deficits. To examine this, we tested DLB-AD and control mice in two sensitive cognitive tasks: the BCM and IA (Barnes, 1979).

Barnes circular maze

Non-Tg, M83-h, 3xTg-AD, and DLB-AD mice were trained on the BCM task at 2, 4, 6, 9, and 12 months of age following standard protocols, and the resultant acquisition curves were used to compare spatial recognition memory. At 2 months of age, both the 3xTg-AD and DLB-AD mice are significantly impaired compared with age-matched non-Tg and M83-h mice on days 2 and 3 of acquisition (Fig. 1*A*) ($p < 0.05$). By 4 months of age, 3xTg-AD and DLB-AD mice are further impaired, exhibiting significantly longer escape latencies than non-Tg and M83-h mice across all 4 d of acquisition.

Importantly, by 6 months of age, DLB-AD mice perform significantly worse than age-matched 3xTg-AD mice (Fig. 1*A*) ($p < 0.05$). This marked acceleration of cognitive decline in DLB-AD mice becomes even further pronounced by 9 months of age. In contrast, by 12 months of age, 3xTg-AD and DLB-AD mice exhibit similarly robust deficits in acquisition. Interestingly, at 12 months of age, M83-h single-transgenic mice are also impaired during acquisition, in line with recent evidence that mutant α-syn alone can impair cognition (Freichel et al., 2007). Importantly, all ages and genotypes are unimpaired on the cued version of the BCM; thus, impairments in BCM acquisition result not from differences in motivation, vision, or motor ability, but rather from deficits in spatial memory (Fig. 1*B*) ($p > 0.05$).

After BCM acquisition, we also tested retention based on escape latency using a single trial at 24 h and 7 d after the last training trial. We found that 2-month-old 3xTg-AD and DLB-AD mice have significantly longer escape latencies compared with age-matched non-Tg and M83-h mice at the 24 h retention trial (Fig. 1*C*) ($p < 0.05$). However, all four genotypes are indistinguishable at the 7 d retention trial (Fig. 1*C*) ($p > 0.05$). At 4 months of age, 3xTg-AD and DLB-AD mice are significantly impaired compared with age-matched non-Tg and M83-h mice during both the 24 h and 7 d retention trials (Fig. 1*C*) ($p < 0.05$).

Similar to our findings during BCM acquisition, we found that during the 24 h retention trial, 6-month-old DLB-AD mice exhibited significantly longer escape latencies compared with 3xTg-AD mice (Fig. 1*C*) ($p < 0.05$). Thus, coexpression of mutant α-syn exacerbates cognitive deficits not only in the acquisition of spatial recognition memory but also in the retention of memory. At 9 months, the 3xTg-AD and DLB-AD mice are significantly worse than age-matched non-Tg and M83-h mice at the 24 h and 7 d retention trials, and the DLB-AD mice are further impaired than 3xTg-AD mice during both retention trials (Fig. 1*C*) ($p < 0.05$). By 12 months of age, 3xTg-AD and DLB-AD mice remain significantly impaired versus non-Tg and M83-h mice on both retention trials, but no longer exhibit differences in performance between each other, suggestive of a ceiling effect (Fig. 1*C*) ($p < 0.05$).

In addition to recording escape latency, we also quantified the number of incorrect holes (errors) visited by animals during BCM acquisition. This is an important additional measure as an animal's affinity to explore a novel environment can influence BCM acquisition. Importantly, we found no differences in the number of incorrect holes visited (i.e., exploration of the maze) on day 1 of training for any age from 2 to 12 months of age (Fig. 1*D*). Thus, there are no differences in the general exploratory

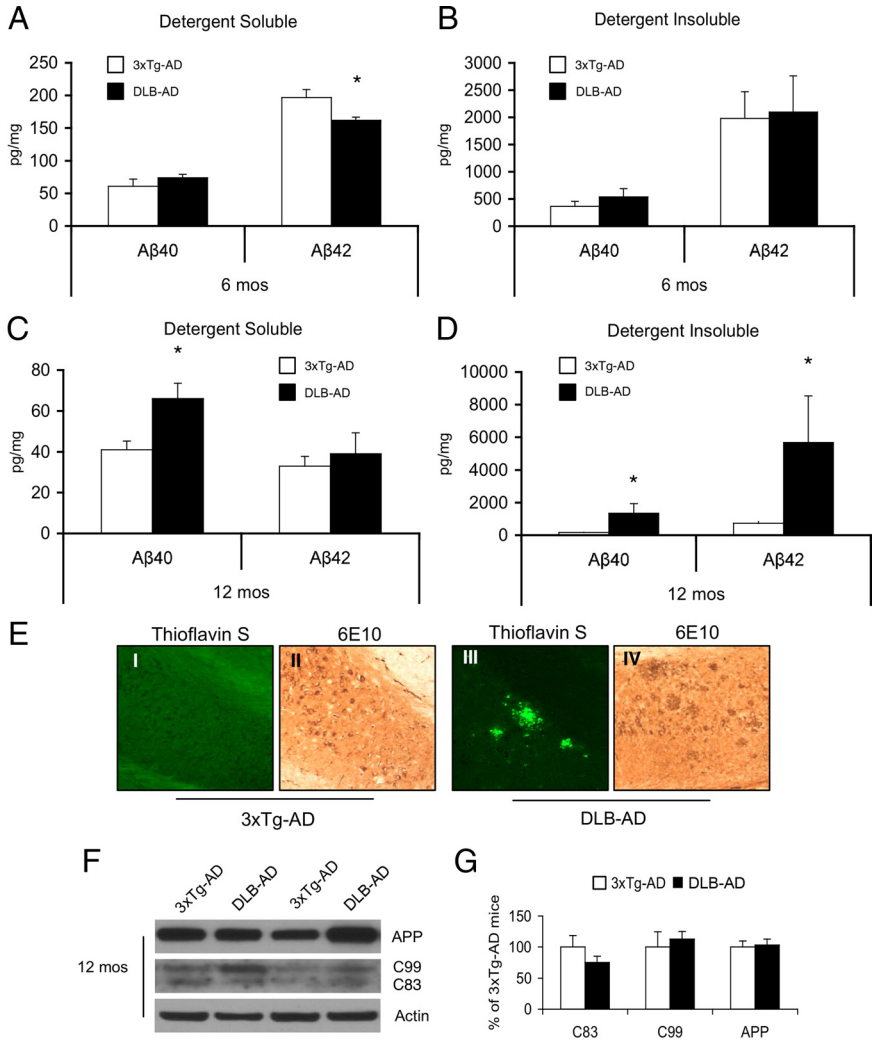

Figure 3. Aβ solubility and plaque load is increased in the DLB-AD mice. ***A***, Detergent-soluble whole-brain $A\beta_{42}$ in 6-month-old DLB-AD compared with age-matched 3xTg-AD mice ($*p < 0.05$); no change in soluble $A\beta_{40}$. ***B***, No change in detergent-insoluble $A\beta_{40}$ and $A\beta_{42}$ ($p > 0.05$). ***C***, Detergent-soluble $A\beta_{40}$ is increased in 12-month-old DLB-AD mice compared with age-matched 3xTg-AD mice ($*p < 0.05$); no change in $A\beta_{42}$. ***D***, Detergent-insoluble whole-brain $A\beta_{40}$ and $A\beta_{42}$ levels are significantly increased in DLB-AD mice compared with age-matched 3xTg-AD mice ($*p < 0.05$). ***E***, Twelve-month-old DLB-AD mice have more plaques based on 6E10 immunoreactivity and many of these plaques are thioflavin S positive. ***F***, Steady-state levels of APP, C99, and C83 are comparable between 12-month-old 3xTg-AD and DLB-AD mice, and quantification (***G***) reveals no significant differences ($p > 0.05$). Error bars indicate SEM.

activity of these groups. As unimpaired (i.e., non-Tg) animals learn the BCM task, the number of errors decreases with each subsequent day of training. This pattern is especially apparent in 2-month-old animals, in which all genotypes reach the same escape latency by day 4 of training. However, when animals do not acquire the spatial location of the escape box, they continue to make a high number of errors as they continue to search for the escape box. As previously discussed, 4-month-old 3xTg-AD and DLB-AD mice are impaired on acquisition (Fig. 1*A*), and they also exhibit significantly more errors compared with age-matched non-Tg and M83-h mice (Fig. 1*D*). Interestingly, 6-month-old DLB-AD mice make significantly more errors on day 4 than all three other genotypes (Fig. 1*D*), consistent with the pronounced deficits in acquisition and escape latency that also occur at this age. By 9 months of age, DLB-AD mice continue to make significantly more errors than the non-Tg and M83-h mice on days 3 and 4; however, they are no longer significantly different from age-matched 3xTg-AD mice. At 12 months of age, both the 3xTg-AD and DLB-AD mice continue to make significantly more errors compared with the non-Tg and M83-h mice on day 4 of acquisition (Fig. 1*D*) ($p < 0.05$). Together, these data demonstrate that the coexpression of mutant α-syn exacerbates cognitive deficits in 3xTg-AD mice.

In addition to BCM, which is primarily a spatial, hippocampal-dependent task, we also tested the mice on IA, a task that is more dependent on the basal lateral amygdala. We found that deficits on IA appear later than BCM as all genotypes perform equivalently at 2 and 4 months of age (Fig. 2) ($p > 0.05$). In contrast, 6- and 9-month-old DLB-AD mice cross over into the dark (shock) compartment significantly earlier than age-matched non-Tg, M83-h, and 3xTg-AD mice at the 1.5 h probe, indicating reduced memory for having previously received a shock (Fig. 2) ($p < 0.05$). At the 24 h probe, there are no longer any differences between DLB-AD and 3xTg-AD mice at either 6 or 9 months of age. However, DLB-AD mice remain significantly impaired versus non-Tg and M83-h groups at these ages. By 12 months of age, both 3xTg-AD and DLB-AD mice are significantly impaired versus age-matched non-Tg and M83-h mice during both probe trials (Fig. 2) ($p < 0.05$).

It is not surprising the deficits in the 3xTg-AD and DLB-AD mice occur later in the IA task compared with the BCM. IA involves a simple, one-trial learning paradigm, whereas the BCM is a much more complicated and difficult task to acquire. Interestingly, the DLB-AD mice are significantly more impaired compared with age-matched 3xTg-AD mice at several time points on both the BCM and IA. This fits well with the clinical finding that the disease course in DLB-AD patients is often more aggressive and cognitive deficits are more severe than in pure AD (Hansen et al., 1990; Langlais et al., 1993).

Exacerbated Aβ and plaque pathology in DLB-AD mice

To determine the mechanism by which cognitive decline is accelerated in DLB-AD mice, we examined the neuropathological progression of plaque, tangle, and LB pathology using both histological and biochemical approaches. Aβ accumulation correlates well with cognitive decline in the 3xTg-AD mice (Billings et al., 2005); thus, we began by quantifying detergent-soluble and -insoluble Aβ using ELISA. Six-month-old DLB-AD mice exhibit a small but significant decrease in detergent-soluble $A\beta_{42}$ compared with age-matched 3xTg-AD mice (Fig. 3*A*) ($p < 0.05$). In contrast, there were no significant changes in detergent-insoluble Aβ (Fig. 3*B*) ($p > 0.05$). However, by 12 months of age, DLB-AD mice display a marked increase in detergent-insoluble $A\beta_{40}$ and $A\beta_{42}$ as well as an increase in detergent-soluble $A\beta_{40}$ compared with age-matched 3xTg-AD mice (Fig. 3*C*,*D*) ($p < 0.05$). The

increase in insoluble Aβ peptides in 12-month-old DLB-AD mice correlate well with the appearance of thioflavin-positive dense-core plaques within the subiculum. In contrast, strain-matched 3xTg-AD mice exhibit only occasional diffuse plaques within the hippocampus by this age (Fig. 3*E*), significantly less plaques than the DLB-AD mice ($p > 0.05$).

Previous work from our laboratory suggests that Aβ plaques begin to appear in the hippocampus at 12 months of age in 3xTg-AD mice (Oddo et al., 2003). In contrast, the 3xTg-AD mice used in this study start to exhibit plaques at later time points, likely as a result of altered background strain. Indeed, studies have shown that background strains can dramatically affect APP processing and Aβ biogenesis (Lehman et al., 2003). The 3xTg-AD mice used in this study were derived during the same crosses that generated the DLB-AD mice to control for any possible effect of background strain.

We next investigated whether APP processing was altered in the DLB-AD mice. As shown, we find no differences in the steady-state levels of APP or its derivatives, C99 or C83, in 12-month-old DLB-AD mice (Fig. 3*F*,*G*).

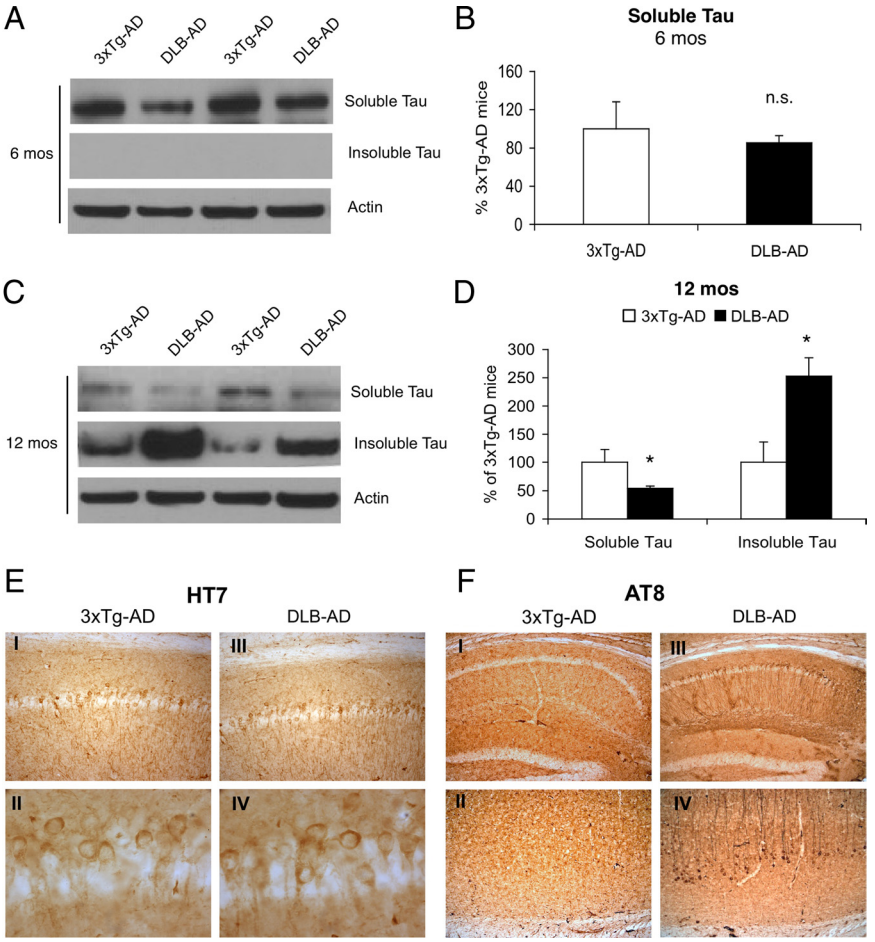

Figure 4. Tau solubility and phosphorylation is exacerbated in the DLB-AD mice. ***A***, There are no differences in soluble steady-state tau levels in 6-month-old 3xTg-AD and DLB-AD. There is also no insoluble tau at this age. ***B***, Quantification of soluble tau levels indicates there are no differences in steady-state levels ($p > 0.05$). ***C***, Soluble steady-state tau levels appear to decrease in 12-month-old DLB-AD mice with a concomitant increase in detergent-insoluble tau. ***D***, Quantification of steady-state soluble and insoluble tau indicates there is a significant decrease and increase, respectively, in 12-month-old DLB-AD mice compared with age-matched 3xTg-AD mice (*$p < 0.05$). ***E***, 3xTg-AD and DLB-AD mice exhibit somatodendritic tau accumulation in the septal CA1 (I and III, respectively), and the morphology of the tau accumulation appears to be indistinguishable as shown at higher magnification (II vs IV). ***F***, There are no AT8-postive cells in the septal CA1 of the hippocampus in the 3xTg-AD mice (shown in I), whereas there are AT8-positive tangles in the same region of the DLB-AD mice (shown in III). There is a similar disparity in the neocortex where AT8 cells are not apparent in the 3xTg-AD mice, but AT8-positive tangles are present in the DLB-AD mice (II and IV, respectively). Error bars indicate SEM.

Acceleration of tau pathology in DLB-AD mice

α-syn has been shown to be enhance tau aggregation and phosphorylation both *in vitro* and *in vivo* (Giasson et al., 2003; Frasier et al., 2005). We therefore examined the accumulation, phosphorylation, and aggregation of tau in the DLB-AD mice. Six-month-old DLB-AD mice exhibit no change in detergent-soluble total human tau versus 3xTg-AD mice (Fig. 4*A*,*B*) ($p > 0.05$). At this age, detergent-insoluble tau is absent in both groups (Fig. 4*A*). By 12 months of age, DLB-AD mice demonstrate a significant decrease in detergent-soluble tau and a corresponding increase in detergent-insoluble tau (Fig. 4*C*,*D*) ($p < 0.05$). Although the spatial localization of HT7 tau remains unaltered in 12-month-old mice (Fig. 4*E*), there is a dramatic increase in phospho-tau (AT8) immunoreactivity (Fig. 4*F*). Twelve-month-old 3xTg-AD mice exhibit few AT8-positive cells within the dorsoventral aspect of CA1 and the neocortex (Fig. 4*F*, I, II). In contrast, age-matched DLB-AD mice exhibit substantial AT8 immunoreactivity within these regions (Fig. 4*F*, III, IV).

Pathological changes in α-syn and LB-like deposits are accelerated in DLB-AD mice

Changes in α-syn solubility appear to temporally precede changes in tau solubility as 6-month-old DLB-AD mice accumulate detergent-insoluble α-syn (Fig. 5*A*,*B*) ($p < 0.05$). In contrast, the single-transgenic M83-h mice express equivalent levels of α-syn transgene, but detergent-insoluble α-syn does not accumulate until 22–28 months of age. Previous studies have shown that homozygous M83 mice develop detergent-insoluble α-syn between 8 and 16 months of age (Giasson et al., 2002). Thus, it is notable that concurrent expression of Aβ and tau in DLB-AD mice can trigger the deposition of detergent-insoluble α-syn by 6 months of age, despite only heterozygous α-syn expression.

In Lewy body diseases, α-syn undergoes several posttranslational modifications including phosphorylation at serine 129 (pS129). Interestingly, pS129 is found almost exclusively in LBs (Fujiwara et al., 2002), and pS129 α-syn enhances the formation of eosinophilic cytoplasmic inclusions in SH-SY5Y cells (Smith et al., 2005). Thus, we examined whether α-syn is preferentially phosphorylated at S129 in the DLB-AD mice. At 6 months of age, there is a nonsignificant trend toward an increase in detergent-soluble α-syn and pS129 α-syn (Fig. 5*A*,*B*) ($p > 0.05$). However, by 12 months of age, soluble pS129 levels are significantly elevated in DLB-AD mice compared with age-matched M83-h and 3xTg-AD mice (Fig. 5*C*,*D*) ($p < 0.05$). At this age, pS129 α-syn is also detected within the insoluble fraction (Fig. 5*C*). Importantly, only 12-month-old DLB-AD mice exhibit high-molecular-

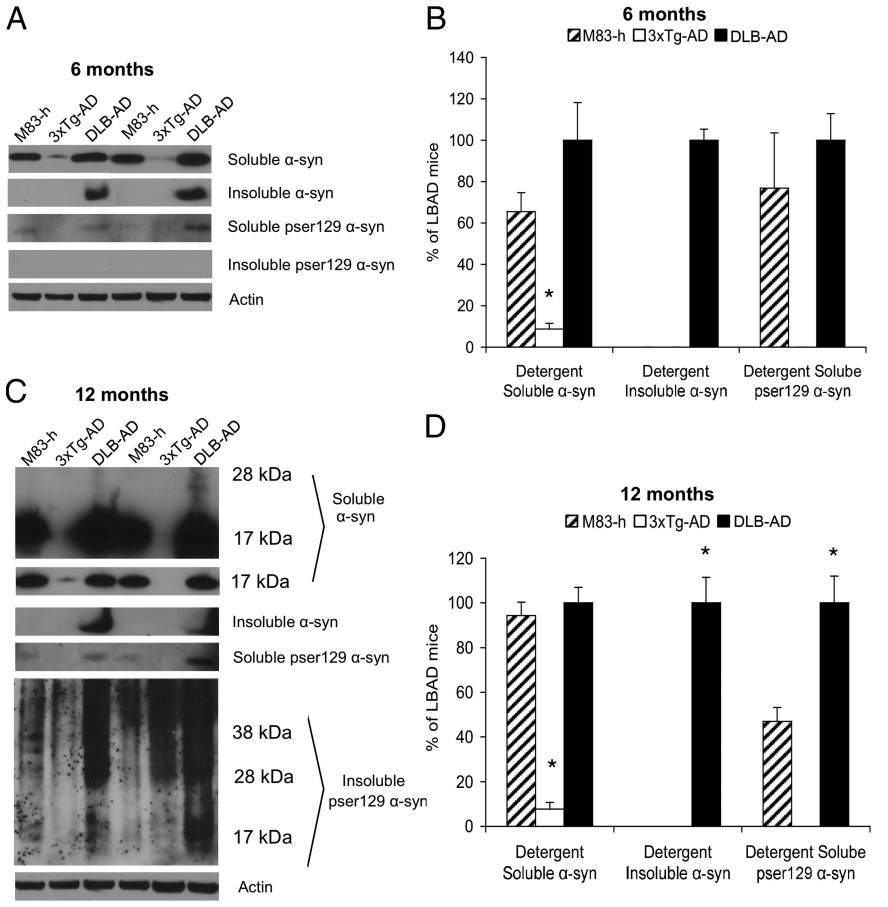

Figure 5. α-syn accumulation, solubility, and phosphorylation is altered in the DLB-AD mice. ***A***, Comparison of soluble and insoluble α-syn and pS129 α-syn in 6-month-old M83-h, 3xTg-AD, and DLB-AD mice. ***B***, Significantly more detergent-soluble α-syn in both the M83-h and DLB-AD mice compared with age-matched 3xTg-AD mice (*$p < 0.05$). Significantly, detergent-insoluble α-syn is present in DLB-AD mice but absent in both M83-h and 3xTg-AD mice. ***C***, Soluble and insoluble α-syn and pS129 α-syn in 12-month-old M83-h, 3xTg-AD, and DLB-AD mice. ***D***, Significantly more detergent-soluble α-syn in both the M83-h and DLB-AD mice compared with age-matched 3xTg-AD mice (*$p < 0.05$). There is also the appearance of high-molecular-weight α-syn that is only apparent in the DLB-AD mice. Insoluble α-syn is still only apparent in the DLB-AD mice (*$p < 0.05$). Soluble pS129 levels are significantly increased in the DLB-AD mice compared with age-matched M83-h and 3xTg-AD mice (*$p < 0.05$). Error bars indicate SEM.

weight soluble α-syn species and accumulate detergent-insoluble α-syn (Fig. 5*C*,*D*) ($p < 0.05$). This exciting finding suggests that Lewy body-like pathology begins to manifest in 12-month-old DLB-AD mice, long before it appears in M83-h single transgenics.

Indeed, the observed biochemical changes in α-syn are reflected *in situ* as the accumulation and distribution of LB-like inclusions are significantly accelerated in the DLB-AD mice. Our hypothesis posited that synergistic amyloidogenic interactions of Aβ and tau would accelerate the formation of LB-like inclusions. M83-h mice develop LB-like inclusions by 28 months of age, whereas homozygous M83 mice develop LB-like inclusions at 8–16 months of age (Giasson et al., 2002), primarily in the pons, spinal cord, and other hindbrain regions; we also found a paucity of LB-like inclusions in 24-month-old hemizygous M83 mice (Fig. 6*A*). In contrast, the formation of LB-like inclusions is accelerated in the DLB-AD mice as they develop diffuse LB-like inclusions at 12 and 18 months of age in the cortex (Fig. 6*B*,*C*). Interestingly, examples of neurons that colocalize both α-syn and Aβ immunoreactivity are also observed at 12 months of age (supplemental Fig. 3*G–L*, available at www.jneurosci.org as supplemental material). Small LB-like α-syn inclusions are also present in the septum in 18-month-old DLB-AD mice (data not shown), and within the subiculum (Fig. 6*K–T*), two regions that are critical for spatial learning and memory. By 24 months of age, dense LB-like inclusions are readily apparent in DLB-AD mice (Fig. 6*D*), and these α-syn-immunoreactive aggregates resemble human LBs (Fig. 6*E*). The 3xTg-AD mice do not appear to develop LBs, but some α-syn does accumulate around plaques in 18-month-old mice (Fig. 6*F–J*). In contrast, all three pathologies, plaques, tangles, and LB-like inclusions, are observed in 18-month-old DLB-AD mice within the subiculum (Fig. 6*K–T*; supplemental Fig. 3*M–R*, available at www.jneurosci.org as supplemental material). Together, these data support the notion that Aβ, tau, and α-syn can synergistically exacerbate the aggregation and deposition of each other, thereby promoting the additional acceleration of cognitive decline. A summary of the primary biochemical findings is provided in Table 1.

To explore the possibility that neuronal injury or altered inflammatory response might contribute to the phenotype of DLB-AD mice, we immunolabeled a subset of brains for the neuronal marker NeuN, the astrocytic marker, GFAP, and the microglial marker IBA-1. As shown in supplemental Figure 4 (available at www.jneurosci.org as supplemental material), we see no qualitative differences between DLB-AD and 3xTg-AD mice in neuronal or glial density and morphology.

Discussion

Many patients with AD exhibit LBs in addition to plaques and tangles (Förstl et al., 1993; Hamilton, 2000). A major goal of this experiment was to therefore recapitulate the phenotype of this Lewy body variant of AD and to elucidate the relationships between the three amyloidogenic proteins that produce each lesion, α-syn, Aβ, and tau. To determine the impact of LB pathology on plaque and tangle load, we crossed 3xTg-AD mice with $\alpha\text{-syn}_{A53T}$ transgenic mice (M83). The resulting model is the first, to our knowledge, that exhibits all three brain lesions, modeling both the pathology and the accelerated cognitive decline observed in DLB-AD patients. Importantly, our data also provides powerful *in vivo* evidence that Aβ, tau, and α-syn act synergistically to accelerate the accumulation and aggregation of each other and promote cognitive decline.

One of the most striking and unexpected findings to emerge from this study was the change in Aβ solubility and accumulation. Previous evidence suggests that Aβ, especially $A\beta_{42}$, is very effective at promoting oligomerization of α-syn *in vitro* (Masliah et al., 2001). Masliah et al. also found compelling evidence that Aβ can promote the accumulation of α-syn deposits in transgenic mice *in vivo*. However, there is little previous evidence to suggest that α-syn can in turn promote Aβ accumulation. In this study, we report that there is a dramatic increase in detergent-

insoluble Aβ, especially the more amyloidogenic Aβ_{42} peptide, in 12-month-old DLB-AD mice. These biochemical data are mirrored histopathologically as 12-month-old DLB-AD mice develop dense-core thioflavin S-positive plaques within the subiculum. Aβ_{42} is more prone to form fibrils (Jarrett et al., 1993) and is typically the primary species of Aβ found in plaques (Suzuki et al., 1994). Moreover, recent studies provide compelling evidence that α-syn interacts strongly with Aβ_{42}, causing it to oligomerize and precipitate *in vitro* (Mandal et al., 2006). Our data also suggest that α-syn may directly augment Aβ_{42} accumulation. At younger ages, we observe examples of neurons that accumulate both interneuronal Aβ and intraneuronal α-syn (supplemental Fig. 3*D–L*, available at www.jneurosci.org as supplemental material). Previous studies have shown that a small percentage of newly synthesized α-syn is regularly excreted from the cell via exocytosis (Lee et al., 2005); thus, α-syn may also interact with extracellular Aβ.

There is a great deal of data positing that there is a synergistic relationship between tau and α-syn, and the findings in this paper strongly corroborate this. As previously reported, ~25% of aged M83 transgenic mice develop tau pathology coincident with the accumulation of LB-like deposits (Giasson et al., 2003). Overexpression of α-syn$_{A30P}$ in transgenic mice also promotes tau phosphorylation (Frasier et al., 2005). Here, we demonstrate that there is a marked acceleration of AT8-immunoreactive tau deposition within the hippocampus and cortex of DLB-AD mice. It is difficult to precisely determine whether the increase in tau pathology observed in DLB-AD mice is mediated directly via α-syn versus indirectly via increased Aβ pathology. However, the earliest pathological change detected in the DLB-AD mice is the accumulation of detergent-insoluble α-syn at 6 months of age, suggesting that α-syn likely directly affects tau pathology.

Phosphorylation of α-syn at S129 may be a significant pathological event as α-syn is not commonly phosphorylated at this residue under physiological conditions (Okochi et al., 2000; Fujiwara et al., 2002). Only ~4% of α-syn is phosphorylated at this site within the normal rat brain, whereas 90% of α-syn is phosphorylated at S129 in synucleinopathies such as dementia with LBs, and pS129 α-syn can promote fibril formation *in vitro* (Fujiwara et al., 2002). We provide evidence to suggest that pathological changes in Aβ and tau are associated with a concomitant increase in α-syn S129 phosphorylation *in vivo*. S129 α-syn is observed first within the soluble fraction at 6 months of age, whereas by 12 months S129 α-syn also appears within the insoluble fraction of DLB-AD mice. Casein kinases 1 and 2 (CK1, CK2) have been identified as the primary kinases involved in S129 phosphorylation of α-syn (Okochi et al., 2000). Interestingly, CK1 expression levels are increased in the brains of AD patients (Yasojima et al., 2000). Thus, altered CK activity may play a role in the enhanced phosphorylation of S129 observed in DLB-AD mice versus M83-h single-transgenic mice. In summary, our data provide compelling evidence that Aβ, tau, and α-syn synergize to promote the aggregation, phosphorylation, and accumulation of each other and to accelerate cognitive decline.

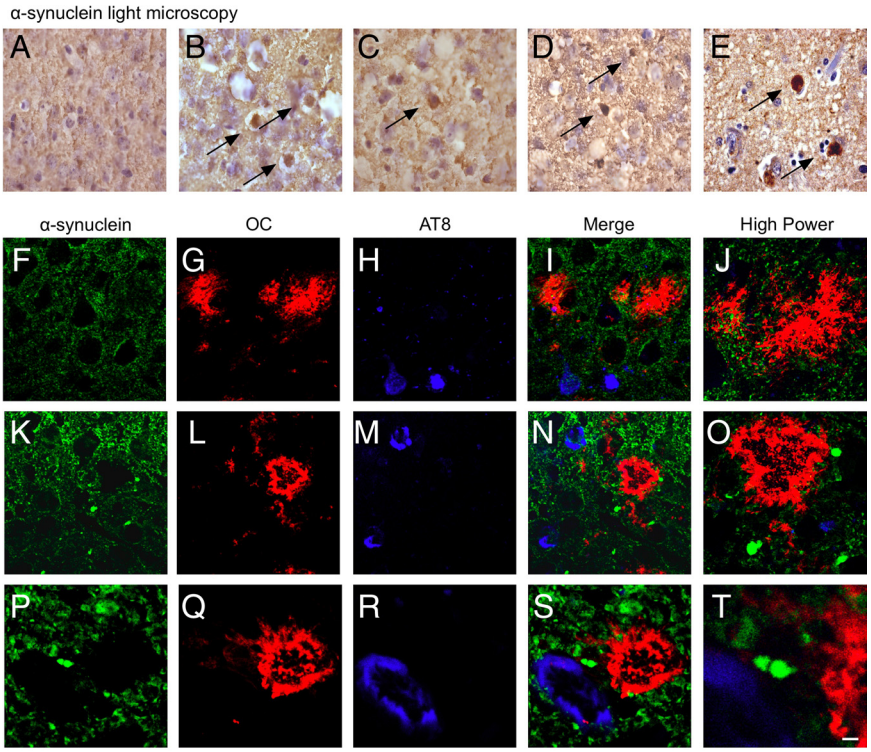

Figure 6. LB-like pathology is increased by coexpression of APP and tau. Normal neuropil staining of α-syn in 24-month-old M83-h brain (representative photomicrograph from the cortex) is shown in ***A***. Twelve-, 18-, and 24-month-old DLB-AD mice develop LB-like inclusions in the cortex as depicted in ***B–D***, respectively. Representative human LB is shown in ***E***. Eighteen-month-old 3xTg-AD mice maintain normal neuropil staining of α-syn despite the development of plaques and AT8-positive cells (***F–J***). Eighteen-month-old DLB-AD mice develop LB-like deposits, plaques, and AT8-positive cells in the subiculum (***K–T***). Scale bar: ***F–I***, ***K–N***, 12 μm; ***A–E***, ***J***, ***O***, 5 μm; ***P–S***, 2.5 μm; ***T***, 0.6 μm.

Table 1. Summary of biochemical analyses of Aβ, tau, and α-syn in DLB-AD and 3xTg-AD mice at 6 and 12 months of age

		Genotype	
Age	Pathology	3xTg-AD	DLB-AD
6 months	Tau (soluble)	+	+
	Tau (insoluble)	−	−
	α-syn (soluble)	+	++++
	α-syn (insoluble)	−	++++
	pser-129 (soluble)	−	++++
	pser-129 (insoluble)	−	−
	Aβ40 (soluble)	+	+
	Aβ42 (soluble)	+++	++
	Aβ40 (insoluble)	+	+
	Aβ42 (insoluble)	++	++
12 months	Tau (soluble)	++	+
	Tau (insoluble)	+	++
	α-syn (soluble)	+	+++++
	α-syn (insoluble)	−	+++++
	pser-129 (soluble)	−	++++
	pser-129 (insoluble)	++	+++
	Aβ40 (soluble)	+	++
	Aβ42 (soluble)	+	+
	Aβ40 (insoluble)	+	+++
	Aβ42 (insoluble)	+	++++

Relative levels of pathology are indicated by "+" signs, whereas "−" indicates undetectable levels.

References

Barnes CA (1979) Memory deficits associated with senescence: a neurophysiological and behavioral study in the rat. J Comp Physiol Psychol 93:74–104.

Billings LM, Oddo S, Green KN, McGaugh JL, LaFerla FM (2005) Intraneuronal Abeta causes the onset of early Alzheimer's disease-related cognitive deficits in transgenic mice. Neuron 45:675–688.

Blurton-Jones M, Tuszynski MH (2006) Estradiol-induced modulation of estrogen receptor-beta and GABA within the adult neocortex: a potential transsynaptic mechanism for estrogen modulation of BDNF. J Comp Neurol 499:603–612.

Clinton LK, Billings LM, Green KN, Caccamo A, Ngo J, Oddo S, McGaugh JL, LaFerla FM (2007) Age-dependent sexual dimorphism in cognition and stress response in the 3xTg-AD mice. Neurobiol Dis 28:76–82.

Förstl H, Burns A, Luthert P, Cairns N, Levy R (1993) The Lewy-body variant of Alzheimer's disease. Clinical and pathological findings. Br J Psychiatry 162:385–392.

Frasier M, Walzer M, McCarthy L, Magnuson D, Lee JM, Haas C, Kahle P, Wolozin B (2005) Tau phosphorylation increases in symptomatic mice overexpressing A30P alpha-synuclein. Exp Neurol 192:274–287.

Freichel C, Neumann M, Ballard T, Müller V, Woolley M, Ozmen L, Borroni E, Kretzschmar HA, Haass C, Spooren W, Kahle PJ (2007) Age-dependent cognitive decline and amygdala pathology in alpha-synuclein transgenic mice. Neurobiol Aging 28:1421–1435.

Fujiwara H, Hasegawa M, Dohmae N, Kawashima A, Masliah E, Goldberg MS, Shen J, Takio K, Iwatsubo T (2002) alpha-Synuclein is phosphorylated in synucleinopathy lesions. Nat Cell Biol 4:160–164.

Giasson BI, Duda JE, Quinn SM, Zhang B, Trojanowski JQ, Lee VM (2002) Neuronal alpha-synucleinopathy with severe movement disorder in mice expressing A53T human alpha-synuclein. Neuron 34:521–533.

Giasson BI, Forman MS, Higuchi M, Golbe LI, Graves CL, Kotzbauer PT, Trojanowski JQ, Lee VM (2003) Initiation and synergistic fibrillization of tau and alpha-synuclein. Science 300:636–640.

Hamilton RL (2000) Lewy bodies in Alzheimer's disease: a neuropathological review of 145 cases using alpha-synuclein immunohistochemistry. Brain Pathol 10:378–384.

Hansen L, Salmon D, Galasko D, Masliah E, Katzman R, DeTeresa R, Thal L, Pay MM, Hofstetter R, Klauber M, Rice V, Butters N, Alford M (1990) The Lewy body variant of Alzheimer's disease: a clinical and pathologic entity. Neurology 40:1–8.

Jarrett JT, Berger EP, Lansbury PT Jr (1993) The carboxy terminus of the beta amyloid protein is critical for the seeding of amyloid formation: implications for the pathogenesis of Alzheimer's disease. Biochemistry 32:4693–4697.

Kotzbauer PT, Giasson BI, Kravitz AV, Golbe LI, Mark MH, Trojanowski JQ, Lee VM (2004) Fibrillization of alpha-synuclein and tau in familial Parkinson's disease caused by the A53T alpha-synuclein mutation. Exp Neurol 187:279–288.

Kraybill ML, Larson EB, Tsuang DW, Teri L, McCormick WC, Bowen JD, Kukull WA, Leverenz JB, Cherrier MM (2005) Cognitive differences in dementia patients with autopsy-verified AD, Lewy body pathology, or both. Neurology 64:2069–2073.

Langlais PJ, Thal L, Hansen L, Galasko D, Alford M, Masliah E (1993) Neurotransmitters in basal ganglia and cortex of Alzheimer's disease with and without Lewy bodies. Neurology 43:1927–1934.

Lee HJ, Patel S, Lee SJ (2005) Intravesicular localization and exocytosis of α-synuclein and its aggregates. J Neurosci 25:6016–6024.

Lee VM, Giasson BI, Trojanowski JQ (2004) More than just two peas in a pod: common amyloidogenic properties of tau and alpha-synuclein in neurodegenerative diseases. Trends Neurosci 27:129–134.

Lehman EJ, Kulnane LS, Gao Y, Petriello MC, Pimpis KM, Younkin L, Dolios G, Wang R, Younkin SG, Lamb BT (2003) Genetic background regulates beta-amyloid precursor protein processing and beta-amyloid deposition in the mouse. Hum Mol Genet 12:2949–2956.

Mandal PK, Pettegrew JW, Masliah E, Hamilton RL, Mandal R (2006) Interaction between Abeta peptide and alpha synuclein: molecular mechanisms in overlapping pathology of Alzheimer's and Parkinson's in dementia with Lewy body disease. Neurochem Res 31:1153–1162.

Masliah E, Rockenstein E, Veinbergs I, Sagara Y, Mallory M, Hashimoto M, Mucke L (2001) β-Amyloid peptides enhance α-synuclein accumulation and neuronal deficits in a transgenic mouse model linking Alzheimer's disease and Parkinson's disease. Proc Natl Acad Sci U S A 98:12245–12250.

Oddo S, Caccamo A, Shepherd JD, Murphy MP, Golde TE, Kayed R, Metherate R, Mattson MP, Akbari Y, LaFerla FM (2003) Triple-transgenic model of Alzheimer's disease with plaques and tangles: intracellular Abeta and synaptic dysfunction. Neuron 39:409–421.

Oddo S, Billings L, Kesslak JP, Cribbs DH, LaFerla FM (2004) Abeta immunotherapy leads to clearance of early, but not late, hyperphosphorylated tau aggregates via the proteasome. Neuron 43:321–332.

Oddo S, Caccamo A, Tran L, Lambert MP, Glabe CG, Klein WL, LaFerla FM (2006) Temporal profile of amyloid-beta (Abeta) oligomerization in an in vivo model of Alzheimer disease. A link between Abeta and tau pathology. J Biol Chem 281:1599–1604.

Okochi M, Walter J, Koyama A, Nakajo S, Baba M, Iwatsubo T, Meijer L, Kahle PJ, Haass C (2000) Constitutive phosphorylation of the Parkinson's disease associated alpha-synuclein. J Biol Chem 275:390–397.

Olichney JM, Galasko D, Salmon DP, Hofstetter CR, Hansen LA, Katzman R, Thal LJ (1998) Cognitive decline is faster in Lewy body variant than in Alzheimer's disease. Neurology 51:351–357.

Postina R (2008) A closer look at alpha-secretase. Curr Alzheimer Res 5:179–186.

Raghavan R, Khin-Nu C, Brown A, Irving D, Ince PG, Day K, Tyrer SP, Perry RH (1993) Detection of Lewy bodies in trisomy 21 (Down's syndrome). Can J Neurol Sci 20:48–51.

Smith WW, Margolis RL, Li X, Troncoso JC, Lee MK, Dawson VL, Dawson TM, Iwatsubo T, Ross CA (2005) α-Synuclein phosphorylation enhances eosinophilic cytoplasmic inclusion formation in SH-SY5Y cells. J Neurosci 25:5544–5552.

Suzuki N, Cheung TT, Cai XD, Odaka A, Otvos L Jr, Eckman C, Golde TE, Younkin SG (1994) An increased percentage of long amyloid beta protein secreted by familial amyloid beta protein precursor (beta APP717) mutants. Science 264:1336–1340.

Trojanowski JQ (2002) "Emerging Alzheimer's disease therapies: focusing on the future." Neurobiol Aging 23:985–990.

Tsigelny IF, Crews L, Desplats P, Shaked GM, Sharikov Y, Mizuno H, Spencer B, Rockenstein E, Trejo M, Platoshyn O, Yuan JX, Masliah E (2008) Mechanisms of hybrid oligomer formation in the pathogenesis of combined Alzheimer's and Parkinson's diseases. PLoS ONE 3:e3135.

Yamasaki TR, Blurton-Jones M, Morrissette DA, Kitazawa M, Oddo S, LaFerla FM (2007) Neural stem cells improve memory in an inducible mouse model of neuronal loss. J Neurosci 27:11925–11933.

Yasojima K, Kuret J, DeMaggio AJ, McGeer E, McGeer PL (2000) Casein kinase 1 delta mRNA is upregulated in Alzheimer disease brain. Brain Res 865:116–120.